Acid sphingomyelinase deficiency protects mitochondria and improves function recovery after brain injury

Sergei A. Novgorodov,* Joshua R. Voltin,* Wenxue Wang,† Stephen Tomlinson,† Christopher L. Riley,§ and Tatyana I. Gudz[1,*,§]

Departments of Neuroscience* and Microbiology and Immunology,† Medical University of South Carolina, Charleston, SC 29425; and Ralph H. Johnson Veterans Affairs Medical Center,§ Charleston, SC 29401

Abstract **Traumatic brain injury (TBI) is one of the leading causes of disability worldwide and a prominent risk factor for neurodegenerative diseases. The expansion of nervous tissue damage after the initial trauma involves a multifactorial cascade of events, including excitotoxicity, oxidative stress, inflammation, and deregulation of sphingolipid metabolism that further mitochondrial dysfunction and secondary brain damage. Here, we show that a posttranscriptional activation of an acid sphingomyelinase (ASM), a key enzyme of the sphingolipid recycling pathway, resulted in a selective increase of sphingosine in mitochondria during the first week post-TBI that was accompanied by reduced activity of mitochondrial cytochrome oxidase and activation of the Nod-like receptor protein 3 inflammasome. TBI-induced mitochondrial abnormalities were rescued in the brains of ASM KO mice, which demonstrated improved behavioral deficit recovery compared with WT mice. Furthermore, an elevated autophagy in an ASM-deficient brain at the baseline and during the development of secondary brain injury seems to foster the preservation of mitochondria and brain function after TBI. Of note, ASM deficiency attenuated the early stages of reactive astrogliosis progression in an injured brain. These findings highlight the crucial role of ASM in governing mitochondrial dysfunction and brain-function impairment, emphasizing the importance of sphingolipids in the neuroinflammatory response to TBI.**—Novgorodov, S. A., J. R. Voltin, W. Wang, S. Tomlinson, C. L. Riley, and T. I. Gudz. **Acid sphingomyelinase deficiency protects mitochondria and improves function recovery after brain injury.** ***J. Lipid Res.*** **2019.** 60: **609–623.**

Supplementary key words sphingolipids • inflammasome • neuroinflammation • astrogliosis

Traumatic brain injury (TBI) is a leading cause of death in older individuals and the major cause of disability among young adults (1, 2). TBI is defined as a disruption of brain structure and physiology due to an extrinsic biomechanical insult triggering neuronal, axonal, and vascular damage (3). Following the primary injury, multiple pathological processes, including oxidative stress, inflammation, energy failure, and changes in neurotransmitter concentrations, contribute to posttraumatic neurologic symptoms such as motor and cognitive deficits (4, 5). Although the severity of the initial brain trauma is the key factor determining the patients' outcome, secondary processes that develop over days and weeks provide an opportunity for clinical intervention (2). Epidemiologic studies have implicated TBI as an important risk factor for developing late-onset Alzheimer's disease (AD) and linked TBI to other neurodegenerative conditions such as Parkinson's disease and amyotrophic lateral sclerosis (6). Emerging evidence suggests that repeated brain injuries among soldiers and athletes could lead to the development of chronic traumatic encephalopathy (CTE) (7). CTE is characterized by the deposition of hyperphosphorylated tau protein and acetylcholine deficiency, which are also the pathological features of AD (8).

Mitochondrial dysfunction appears to be a cardinal feature of the secondary TBI and the centerpiece of multiple converging processes, including glutamate excitotoxicity, oxidative stress, and inflammatory reactions (9). Mitochondria are involved in both the necrotic and apoptotic cell death, which have been reported in animal models (10) and in humans after TBI (11). Mitochondria are known as key players in autophagy, whereby damaged mitochondria are eliminated to maintain proper mitochondrial numbers and quality control. Alterations in the dynamics of autophagy, which can function as a cell-survival mechanism or a mechanism of cell death (lethal autophagy), have been

This work was supported in part by National Institutes of Health Grants R01NS083544 (T.I.G.) and US Department of Veterans Affairs Merit Award I01BX002991 (T.I.G.). The content is solely the responsibility of the authors and does not necessarily represent the official views of the National Institutes of Health.

Manuscript received 14 November 2018 and in revised form 11 January 2019.

Published, JLR Papers in Press, January 20, 2019
DOI https://doi.org/10.1194/jlr.M091132

Abbreviations: 2,4-DNP, 2,4-dinitrophenol; AD, Alzheimer's disease; Aldh1l1, aldehyde dehydrogenase 1 family member L1; ASM, acid sphingomyelinase; CCI, controlled cortical impact; COX, cytochrome oxidase; ECM, extracellular matrix; GFAP, glial fibrillary acidic protein; IL, interleukin; mTOR, mammalian target of rapamycin; MWM, Morris water maze; NCDase, neutral ceramidase; NLRP3, Nod-like receptor P3; NSM, neutral sphingomyelinase; ROS, reactive oxygen species; TBI, traumatic brain injury; TMPD, *N,N,N′,N′*-tetramethyl-*p*-phenelenediamine.

[1]To whom correspondence should be addressed.
e-mail: gudz@musc.edu

observed in the human brain after TBI (12). Mitochondria have been discovered to serve as a platform for Nod-like receptor protein 3 (NLRP3) inflammasome assembly and function (13). The inflammasome is an intracellular multiprotein complex involved in activation of caspase-1, leading to the processing and release of interleukin (IL)-1β and IL-18, which are imperative in the post-TBI neuroinflammatory response (14). Mitochondrial abnormalities [respiratory-chain dysfunction, reactive oxygen species (ROS) production, etc.] are powerful activators of the NLRP3 inflammasome that could also lead to caspase-1-mediated cleavage of the caspase-3/-7, resulting in regulated necrotic cell death (15).

Experimental evidence implicates the disruption of mitochondrial sphingolipid metabolism as an important determinant of the mitochondrial respiratory-chain dysfunction and secondary brain injury after TBI (16). A brain sphingolipidome involves more than 40 enzymes generating and catabolizing dozens of molecular species of sphingolipids, many of which are structural components of the cellular membranes (SMs and gangliosides), whereas bioactive sphingolipids (ceramides, sphingosine, and sphingosine 1-phosphate) play prominent roles in signal transduction governing cell proliferation, differentiation, and programmed cell death (17, 18).

The essential role of sphingosine accumulation as a cause of mitochondrial dysfunction has been demonstrated in a mouse model of TBI (16). The data showed that TBI stimulated the de novo biosynthesis of ceramide in the brain that did not result in an enhanced ceramide level. In fact, ceramide gradually decreased during the first week after TBI, suggesting its augmented conversion into the other sphingolipids, including sphingosine. Further investigation revealed that TBI stimulated mitochondrial neutral ceramidase (NCDase) activity that resulted in an accumulation of mitochondrial sphingosine and mitochondrial dysfunction, promoting secondary brain injury. Sphingosine levels in mitochondria from NCDase KO mice were attenuated by 37% compared with WT mice, suggesting an additional source contributing to mitochondrial sphingosine accumulation in the injured brain. In mammals, sphingosine is generated in a sphingolipid recycling pathway that begins with an acid sphingomyelinase (ASM)-catalyzed SM hydrolysis producing ceramide (19), which is metabolized by an acid ceramidase localized in lysosomes, yielding sphingosine. Transfer of ceramide between intracellular compartments requires either the vesicular transport pathway (20) or nonvesicular mechanisms, including a transfer protein, ceramide transfer protein (21, 22). In contrast, it has been shown that sphingosine can leave the lysosomal compartment and impact mitochondria (23, 24). We hypothesized that TBI could trigger an activation of ASM/acid ceramidase-dependent generation of lysosomal sphingosine, which could reach mitochondria, increasing mitochondrial sphingosine levels and mitochondrial dysfunction, fostering secondary brain injury.

ASM functions in the endolysosomal compartment and on the outer leaflet of the plasma membrane (25), where it facilitates endocytosis and damage repair in the injured cells (26). In apoptosis induced by TNF-α, IFN-γ, and radiation (21, 27), ASM activation led to formation of ceramide-enriched membrane platforms that are central for apoptotic signal transduction (28, 29). ASM/acid ceramidase-dependent mitochondrial sphingosine accumulation was shown to perturb mitochondrial function, which results in regulated necrotic cell death, ferroptosis (24). Of note, an inhibition of ASM activity mediates the effects of antidepressant drugs (30, 31) and diminishes symptoms associated with AD (32).

In this study, we provide evidence for a pivotal role of ASM in mitochondrial dysfunction promoting neuroinflammation and secondary brain injury. Importantly, we show that ASM deficiency (Smpd1 gene ablation) attenuates mitochondrial sphingosine accumulation, preserves mitochondrial function, reduces NLRP3-dependent neuroinflammatory response, and improves brain-function recovery after TBI. These studies suggest a novel mechanism of ASM involvement in the mitochondrial injury linked to neuroinflammation that could be an important factor underlying cognitive deficits after brain trauma.

MATERIALS AND METHODS

Animals and reagents

C57BL6/J (8-week-old) mice (Jackson Laboratory, Bar Harbor, ME) were acclimated for 1 week prior to experimentation. ASM KO mice (C57BL6/J genetic background) were provided by the Animal Core Facility at the Medical University of South Carolina (Charleston, SC). ASM KO ($Smpd1^{-/-}$) mice show age-dependent accumulation of SM and development of Niemann-Pick syndrome A and B (33). We only used the $Smpd1^{-/-}$ mice younger than 12 weeks of age, before any biochemical, histological, or clinical manifestations of Niemann-Pick disease were apparent (34). Experimental protocols were reviewed and approved by the Institutional Animal Care and Use Committee of Ralph H. Johnson VA Medical Center (Charleston, SC) and followed the National Institutes of Health guidelines for experimental animal use. The complete protease inhibitor cocktail and PhosphoStop phosphatase inhibitor cocktail were from Roche Applied Science (Indianapolis, IN). Reclast (zoledronic acid) was from Enzo Biochem (Farmingdale, NY). All other chemicals were purchased from Sigma-Aldrich (St. Louis, MO).

Antibodies

Rabbit monoclonal anti-LC3, anti-beclin-1, anti-NLRP3, and anti-glial fibrillary acidic protein (anti-GFAP) antibodies and rabbit polyclonal anti-p62 antibodies were supplied by Cell Signaling Technology (Danvers, MA). Mouse monoclonal anti-β-actin antibody was from Sigma-Aldrich. Mouse monoclonal anti-caspase-1 and anti-PINK-1 antibodies, as well as rabbit polyclonal anti-ASM antibody were purchased from Santa Cruz Biotechnology (Santa Cruz, CA). Rabbit polyclonal anti-aldehyde dehydrogenase 1 family member L1 (anti-Aldh1l1) antibody was from ThermoFisher (Waltham, MA). Secondary HRP-conjugated antibodies were supplied by Jackson ImmunoResearch (West Grove, PA).

Controlled cortical impact (CCI) injury model of TBI

Mice were anesthetized with isoflurane and placed in a stereotaxic frame (Kopf Instruments, Tujunga, CA). During the surgery, mice maintained a 37°C body temperature by a heating pad.

The skull was exposed, and the bite bar was adjusted to level bregma and lambda in the horizontal plane. The bone over the cortex was removed, exposing a 3.5 mm region at the midline. The impact was delivered by a computer-controlled Head Impactor (Precision Systems and Instrumentation, Fairfax Station, VA) using a 3 mm flat circular impactor tip at a speed of 4 m/s and a depth of 1.5 mm below the cortical surface for 0.1 s The parameter set was to provide a moderate contusive brain injury in mice (16, 35, 36). Sham-injured animals received craniotomy only. After the impact, the wound was sutured, followed by application of analgesic. Mice were placed on the heating pad until ambulatory and then returned to the cage.

Rotarod test

To assess sensorimotor deficits after TBI, the standard rotarod test was performed, as it has been shown to be effective and reliable in rodent brain-trauma experiments (16, 37, 38). The rotarod is a motorized cylinder that accelerates linearly until the animal falls off. Rotarod training and measurement were carried out using a four-lane rotarod apparatus (San Diego Instruments, San Diego, CA). Each day for 3 days prior to injury, animals were trained on the rotarod at a speed of 18 rpm in the acceleration mode (0–18 rpm/90 s). Animals were tested using three trials in each training or measurement session, with a minimum of 5 min resting between trials. One hour before the injury, mice were assessed on the rotarod to obtain preinjury baselines. Scores were measured as the latency or time successfully spent running on the rotarod. Postinjury scores were normalized using preinjury means to control for variability in preinjury performance.

MWM test

To assess spatial learning and retention memory impairments after TBI, a standard Morris water maze (MWM) test was used (39–41). The water maze apparatus consisted of a pool (122 cm diameter) filled with water maintained at 25°C and made opaque with nontoxic white paint. A hidden platform (10 cm diameter) was submerged 1 cm below the water surface. The animals were introduced into the pool at each of four entry points, while the platform location remained constant throughout the training period. Starting points were randomized every day during the 4 day trials. Initial training consisted of four trials per day. On the day of testing, the platform was removed, and the animal's memory-retention abilities were probed by allowing them to free swim for 90 s, and the time spent swimming in each of four quadrants was recorded. The percentage of platform quadrant retention time of the total time was determined. After the swim, mice were warmed and allowed to dry in an incubator at 37°C.

Isolation of mouse-brain mitochondria

All procedures were performed at 4°C as described (42, 43). Mitochondria were isolated from the CCI-injured or sham-injured mouse brain. Briefly, tissue was placed immediately in ice-cold isolation medium containing 230 mM mannitol, 70 mM sucrose, 10 mM HEPES, and 1 mM EDTA, pH 7.4. Brain tissue (~1 g) was homogenized in 10 ml of isolation medium using a Teflon-glass homogenizer. The homogenate was centrifuged at 700 *g* for 10 min. The supernatant was then centrifuged at 10,000 *g* for 10 min. The pellet was resuspended in 2 ml of 15% Percoll-Plus (GE Healthcare, Piscataway, NJ) and placed atop a discontinuous Percoll gradient consisting of a bottom layer of 4 ml of 40% Percoll and a top layer of 4 ml of 20% Percoll. The gradient was spun at 43,000 *g* for 30 min in a SW-Ti41 rotor in a Beckman ultracentrifuge. The fraction at the 20–40% interface, which contained mitochondria, was washed three times with isolation medium (without EDTA) by centrifugation at 10,000 *g* for 10 min. Protein concentration was measured with a bicinchoninic acid assay (Sigma, St. Louis, MO) using BSA as a standard.

Mitochondrial respiratory-chain activity

Mitochondrial respiration was measured by recording oxygen consumption at 25°C in a chamber equipped with a Clark-type oxygen electrode (Instech Laboratories, Plymouth Meeting, PA) as previously described (42, 43). Briefly, mitochondria were incubated in the medium containing 125 mM KCl, 10 mM HEPES, 2 mM KH_2PO_4, 5 mM $MgCl_2$, and 0.5 mg/ml mitochondrial protein supplemented with either complex I substrate (mixture of 5 mM glutamate and 5 mM malate) or complex II substrate (10 mM succinate) in the presence of 5 μM rotenone or complex IV substrate [2 mM ascorbate in the presence of 250 μM *N,N,N′,N′*-tetramethyl-*p*-phenelenediamine (TMPD) and 1 μg/ml antimycin]. A respiratory-control ratio was measured as the oxygen-consumption rate in the presence of the substrate and 500 μM ADP (state 3) divided by the rate in the resting state (state 4) in the presence of 2 μg/ml oligomycin. Uncoupler-stimulated (state 3u) respiration was measured in the presence of 50 μM 2,4-dinitrophenol (2,4-DNP). Cytochrome oxidase (COX) activity was measured as the oxygen-consumption rate supported by COX substrate 2 mM ascorbate with 250 TMPD in the presence of the complex III inhibitor 1 μg/ml antimycin to block the endogenous oxygen consumption.

ASM and NSM activity assay

ASM activity was measured using an ASM activity assay kit (Echelon Biosciences, Salt Lake City, UT) according to the manufacturer's instructions. Synthetic C15-SM was used as a substrate. Neutral sphingomyelinase (NSM) activity was determined as described for the ASM assay, except that the reaction mixture contained 100 mM Tris (pH 7.4) instead of 100 mM sodium acetate (pH 5.0) and was supplemented with 10 mM Mg^{2+}, which is required for NSM activity (44).

Carbonyl content measurement

Protein carbonyls were quantified in mitochondria with the Protein Carbonyl Content Assay Kit (Sigma-Aldrich) according to the manufacturer's instructions.

Western blot

Proteins were analyzed by Western blot (45, 46). Proteins were separated by 4–15% SDS-PAGE, blotted to PVDF membrane, blocked with 5% nonfat dry milk (Bio-Rad, Hercules, CA) or 5% BSA in TBS-T buffer (10 mM Tris, 150 mM NaCl, and 0.2% Tween-20, pH 8.0), and subsequently probed with the appropriate primary antibody. Immunoreactive bands were visualized using a SuperSignal West Dura substrate (ThermoFisher).

Sphingolipid analysis

Sphingolipids content was determined by MS/MS (42, 46). Briefly, to extract lipids, 0.5 mg of mitochondria or brain homogenate protein was added to 2 ml of the ethyl acetate/isopropanol/water (60:30:10%, v/v/v) solvent system. The lipid extracts were fortified with internal standards, dried under a stream of nitrogen gas, and reconstituted in 100 μl of methanol for ESI/MS/MS analysis, which was performed on a ThermoFisher TSQ Quantum triple quadrupole mass spectrometer, operating in a multiple-reaction-monitoring, positive-ionization mode. The samples were injected onto the HP1100/TSQ Quantum LC/MS system and gradient-eluted from the BDS Hypersil C8, 150 × 3.2 mm, 3 μm particle size column, with a 1.0 mM methanolic ammonium formate and 2 mM aqueous ammonium formate mobile-phase

system. The peaks for the target analytes and internal standards were collected and processed with the Xcalibur software system. Calibration curves were constructed by plotting peak area ratios of synthetic standards, representing each target analyte, to the corresponding internal standard. The target analyte peak area ratios from the samples were similarly normalized to their respective internal standard and compared with the calibration curves using a linear regression model. Each sample was normalized to its respective total protein levels.

Statistical analysis

Data were analyzed for statistically significant differences between groups by one-way ANOVA with post hoc analysis or Student's *t*-test where appropriate (SigmaPlot software version 13.0). Statistical significance was ascribed to the data when $P < 0.05$.

RESULTS

TBI triggered ASM activation via posttranscriptional mechanisms

The majority of sphingolipids are extremely hydrophobic; therefore, sphingolipid metabolism is restricted to cellular membranes and is highly compartmentalized (17). De novo sphingolipid biosynthesis occurs in the endoplasmic reticulum and commences with the generation of ceramide, which is then transported to the Golgi and plasma membrane for biosynthesis of SM (17). Another major pathway of sphingolipid metabolism starts with SM hydrolysis and is catalyzed by a sphingomyelinase family enzymes, ASM and NSM, yielding phosphorylcholine and ceramide (47). Hydrophobic ceramide is further hydrolyzed by ceramidase to form more hydrophilic sphingosine, which could leave the intracellular compartment, where it is generated to reach mitochondria (21, 23, 24). ASM is encoded by the Smpd1 gene and translated into 629 amino acid proprotein, which, because of differential modification and trafficking processes, gives rise to two distinct isoforms, lysosomal and secretory ASM (48). The lysosomal ASM resides in the endolysosomal compartment, whereas the secretory ASM is released by the secretory pathway and functions in the extracellular space (26, 49).

To investigate ASM involvement in the secondary brain injury, we used a CCI injury mouse model of TBI that reproduces the neuropathology associated with the multiple types of human TBI (50). Mice were exposed to CCI using a computer-controlled head impactor device to induce the brain injury of moderate severity as described in previous studies (16, 51). Sham-injured mice received craniotomy only. The brain tissue was analyzed at 24, 48, and 168 h (7 days) following the initial insult, and a specific ASM or NSM activity was quantified. **Fig. 1A** shows that TBI triggered a sustained ASM activation during the first week post-TBI, whereas NSM activity did not change. Consistent with our previous proteomic studies (16), there were no changes in the expression level of cerebral ASM protein in response to TBI, indicating the involvement of posttranscriptional mechanisms in ASM activation (Fig. 1B). The data suggest that TBI triggered an activation of ASM-mediated hydrolysis of SM, which could result in an increased generation of sphingosine in the injured brain.

ASM is required for TBI-elicited mitochondrial sphingosine accumulation

We have previously demonstrated a TBI-induced upregulation of sphingosine in brain tissue and cerebral mitochondria that was modestly attenuated in the NCDase-deficient mice (16). To elucidate the role of ASM as a possible source of sphingosine in the brain response to trauma, WT and ASM KO mice were exposed to CCI, and the sphingolipid profile was determined at various time points during the first week post-TBI (**Fig. 2**). Consistent with a previous report, sphingosine levels were elevated in brain tissue up to 181% at 168 h post-TBI compared with sham (Fig. 2A), which was accompanied with slightly attenuated ceramide content up to 76% (Fig. 2B) in WT mice. In the ASM-deficient brain, there were no significant changes in sphingosine or ceramide levels post-TBI compared with sham (Fig. 2A, B). In line with the previous study (16), there was a gradual elevation of sphingosine in WT mitochondria isolated from the injured brain, reaching 246% at 168 h post-TBI compared with sham (Fig. 2C), whereas ceramide was only transiently increased at 24 h, returning to sham levels at 48 h post-TBI (Fig. 2D). No significant changes in mitochondrial sphingosine or ceramide levels were detected in the brains of the ASM KO mice post-TBI compared with sham (Fig. 2C, D). The data suggest that ASM-dependent generation of sphingosine in lysosomes is an important source of mitochondrial sphingosine accumulation during the first week after TBI. It is conceivable that transient elevation of mitochondrial ceramide resulted from lysosomal sphingosine conversion into ceramide by mitochondrial ceramide synthases (43). Given the TBI-induced activation of mitochondrial NCDase (16), the elevated ceramide could be metabolized back into sphingosine at 48 h post-TBI, thereby normalizing ceramide content and increasing sphingosine levels in mitochondria.

TBI-induced mitochondrial dysfunction is rescued in ASM-deficient mice

Sphingosine is a potent endogenous inhibitor of mitochondrial respiratory-chain activity at the level of complex IV in liver (52) and cerebral mitochondria (16). An increased sphingosine content in cerebral mitochondria has been shown to cause a reduced activity of respiratory-chain complex IV (i.e., COX) at 7 days (168 h) post-TBI in WT mice (16). To elucidate the impact of ASM on TBI-induced mitochondrial dysfunction, the respiratory-chain activity was assessed by measuring the oxygen-consumption rate in cerebral mitochondria purified from WT and ASM-deficient mice (**Fig. 3**). The respiratory-chain enzymes transport electrons from the electron donors (substrates) at complex I (glutamate) or complex II (succinate) to complex III and then to complex IV (COX), where the electrons reach their acceptor oxygen. The substrate of complex IV, ascorbate, donates electrons directly to complex IV; therefore, the oxygen-consumption rate supported by ascorbate reflects the activity of the terminal enzyme of the electron

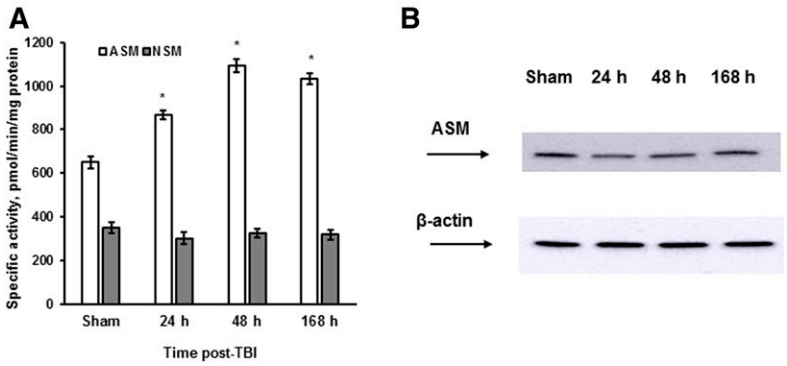

Fig. 1. TBI triggered an activation of ASM via post-transcriptional mechanisms. Brain tissue samples were prepared from the WT mouse brain after the injury imposed by a CCI device. Sham-injured animal brain was used as a control. A: Time course of specific ASM and NSM activity changes was determined. The enzyme activity is expressed as pmol of C15-SM/min per mg of protein. Data are means ± SE. * $P < 0.05$ (n = 10). B: Time course of ASM protein expression changes was assessed following brain trauma. Brain lysates (30 μg/lane) were analyzed by Western blotting using anti-ASM (Santa Cruz) antibody. To confirm equal loading of samples, the membranes were stripped and probed with anti-β-actin antibody. Data are representative of four independent experiments.

transport chain, COX. The addition of 50 μM 2,4-DNP, an uncoupler of oxidative phosphorylation, allowed for the determination of the maximal activity of the respiratory-chain enzymes. In WT mitochondria, there were similar decreases of oxygen-consumption rates supported by either glutamate, succinate, or ascorbate at 24, 48, and 168 h post-TBI compared with sham (Fig. 3A). The data are indicative of TBI-induced blockade of respiratory-chain function at the level of COX that is in line with previous studies (16). To evaluate the impact of ASM on the TBI-induced COX dysfunction, the COX activity was compared in WT and ASM-deficient cerebral mitochondria. In WT mitochondria, COX activity was reduced up to 79% at 24 h and further reduced up to 72% at 48 h, reaching 67% at

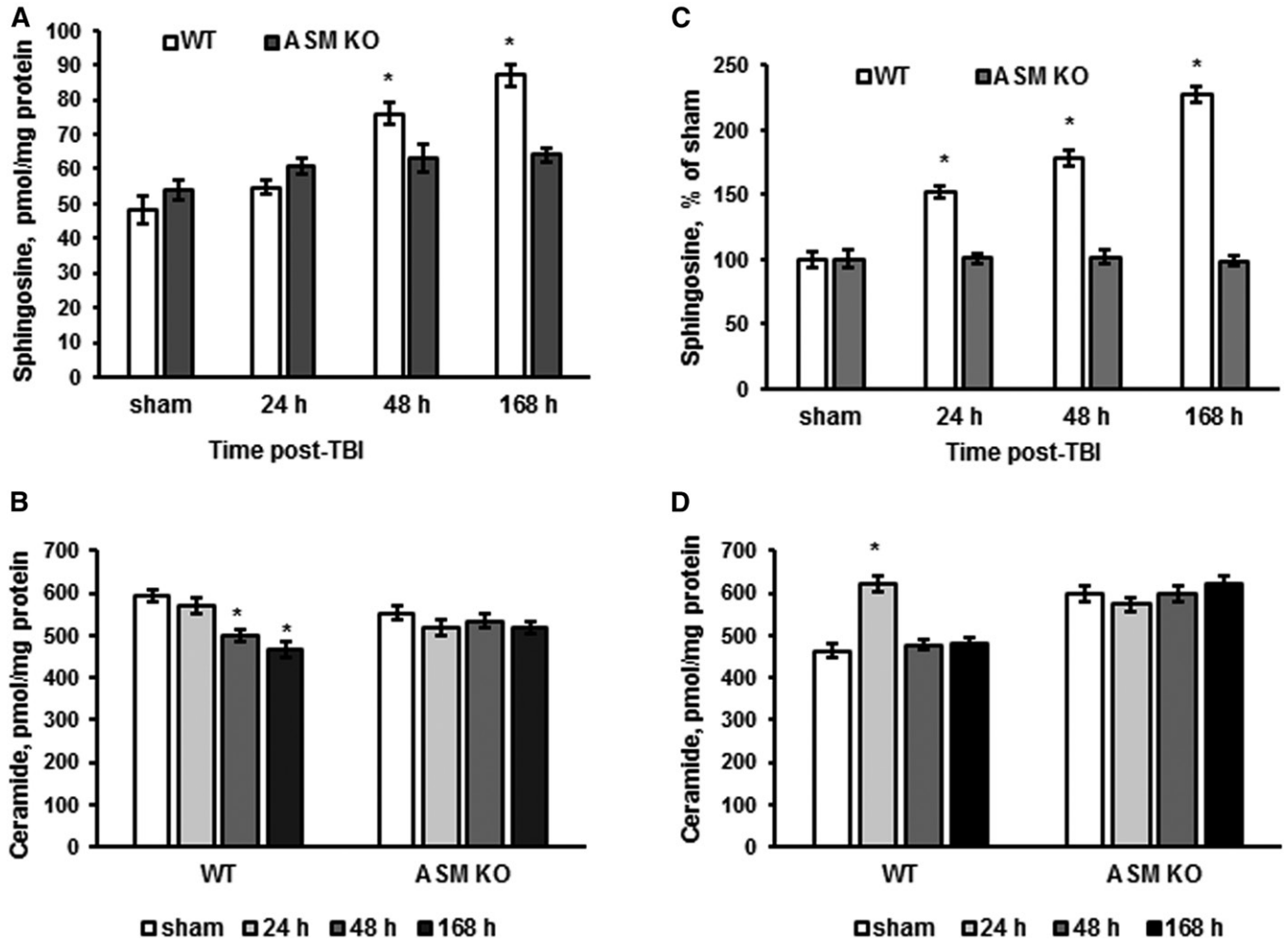

Fig. 2. ASM is required for TBI-induced elevation of sphingosine in mitochondria. Brain tissue and mitochondria samples were prepared from the injured brain of WT and ASM KO mice. Sham-injured animal brain (sham) was used as a control. Sphingosine (A) and ceramide (B) content changes were determined in the brain tissue during the first week post-TBI. Data are means ± SE. * $P < 0.05$ (n = 16). Sphingosine (C) and ceramide (D) content changes were determined in cerebral mitochondria during the first week post-TBI. Data are means ± SE. * $P < 0.05$ (n = 16). Each sample was normalized to its respective total protein levels.

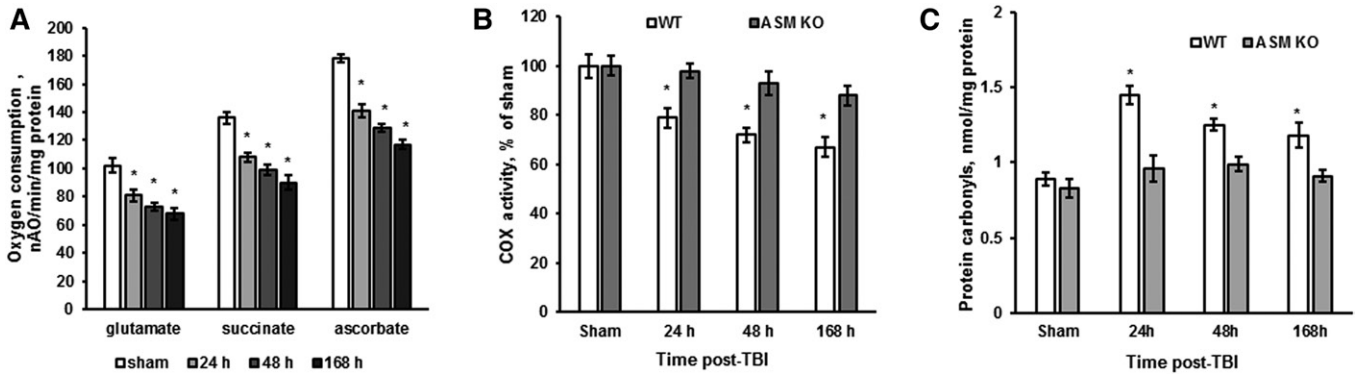

Fig. 3. TBI-induced mitochondrial dysfunction and protein oxidative damage is rescued in the ASM-deficient brain. Mitochondria were purified from the injured brain of WT and ASM KO mice at various time points post-TBI. Sham-injured animal brain (sham) was used as a control. A: Time course of mitochondrial respiration changes was assessed by recording oxygen consumption in the presence of complex I substrate (5 mM glutamate supplemented with 5 mM malate) (glutamate), complex II substrate (10 mM succinate) (succinate), or complex IV (COX) substrate (2 mM ascorbate plus 250 μM TMPD) (ascorbate) and 50 μM 2,4-DNP (State 3u). Data are means ± SE. * $P < 0.05$ (n = 16). nAO, nano atoms oxygen. B: Mitochondrial COX activity was measured by recording oxygen consumption in the presence of COX substrate (2 mM ascorbate plus 250 μM TMPD), 1 μg/ml antimycin, and 50 μM 2,4-DNP. Data are means ± SE. * $P < 0.05$ (n = 16). C: Time course of protein carbonyls changes in mitochondria was determined. Data are means ± SE. * $P < 0.05$ (n = 16).

168 h post-TBI compared with sham (Fig. 3B). COX activity in cerebral mitochondria from ASM-deficient mice at 24, 48, or 168 h post-TBI was not different from the sham (Fig. 3B). The data suggest that TBI-triggered activation of ASM resulted in elevation of mitochondrial sphingosine, which attenuated the maximal COX activity.

It has been shown that a partial suppression of COX activity by cyanide increases mitochondrial ROS formation (53). Moreover, sphingosine-mediated modest inhibition of COX activity enhanced mitochondrial ROS emission in situ (24, 52), which might contribute to oxidative stress, causing an imbalance between oxidant and antioxidant agents in the injured brain (54). Enhanced production of ROS could cause oxidative/nitrosative stress, leading to damage in lipids, proteins, and nucleic acids, known to occur in TBI (55). As a consequence of oxidative stress-mediated proteins modification, the transport of mitochondria to synaptic regions is impaired, which decreases synaptic function and alters signal transduction following TBI (56, 57). To elucidate whether ASM-dependent inhibition of COX leads to augmented protein oxidative modification, protein carbonyl levels were determined in WT and ASM-deficient mitochondria after TBI. The protein carbonyls were higher in WT mitochondria at 24, 48, and 168 h post-TBI (Fig. 3C). ASM knockdown attenuated the TBI-triggered increase in protein carbonyl levels. The data indicate that ASM is necessary for TBI-induced mitochondrial respiratory-chain dysfunction, leading to enhanced oxidative protein modification in the injured brain.

Elevated autophagy in the ASM-deficient brain is augmented after TBI

Having demonstrated ASM involvement in promoting mitochondrial damage in the brain-injury response, we sought to determine the role of ASM in mitochondrial quality-control mechanisms. To curb the accumulation of damaged mitochondria, cells could trigger an elimination of dysfunctional mitochondria by stimulating autophagy and/or mitophagy, an autophagy process facilitated by activation of the PINK-1/Parkin pathway (58). Autophagy, a self-catabolic process by which cells recycle their proteins and organelles in response to stress or injury, has been demonstrated in human injured brain and animal models of TBI (59). Experimental evidence seems to support both a detrimental role of autophagy dysfunction promoting cell death and a protective role for autophagy activators in TBI. A transient elevation of autophagy markers such as Beclin-1 and LC3-II was shown in the mouse cortex at 24 and 48 h post-TBI, whereas the expression of p62 was decreased, signifying an activation of the autophagic flux. Most of the injured cells with enhanced expression of Beclin-1 and LC3-II were positively stained in a TUNEL assay, indicating that elevated autophagy flux was involved in cell death and apoptosis (60). The protective role of autophagy in TBI was demonstrated in studies using rapamycin, an inhibitor of the PIK3/mammalian target of rapamycin (mTOR) signaling pathway. Rapamycin administration to mice augmented the expression of autophagy markers while increasing neuronal survival, reducing inflammation, and improving neurobehavioral function following TBI (61, 62). To investigate ASM involvement in autophagy, the expression of autophagy markers was determined in the injured brain of WT and ASM KO mice at 168 h (7 days) post-TBI (**Fig. 4**). In WT mice, there were no changes in the expression of Beclin-1 and p62, as well as no changes in the expression levels of LC3-I and its lipid-modified form LC3-II. Moreover, there was no change in the expression of the mitophagy marker PINK-1, which has been implicated in the mitophagy failure in Parkinson's disease (58). The data indicate a lack of autophagy involvement in the brain response to injury in WT mice at the end of the first week post-TBI.

Of note, the expression levels of LC3, p62, and Beclin-1 were significantly higher in the ASM-deficient brains of the sham-injured animals compared with WT (Fig. 4). The increased expression of autophagy markers suggests that

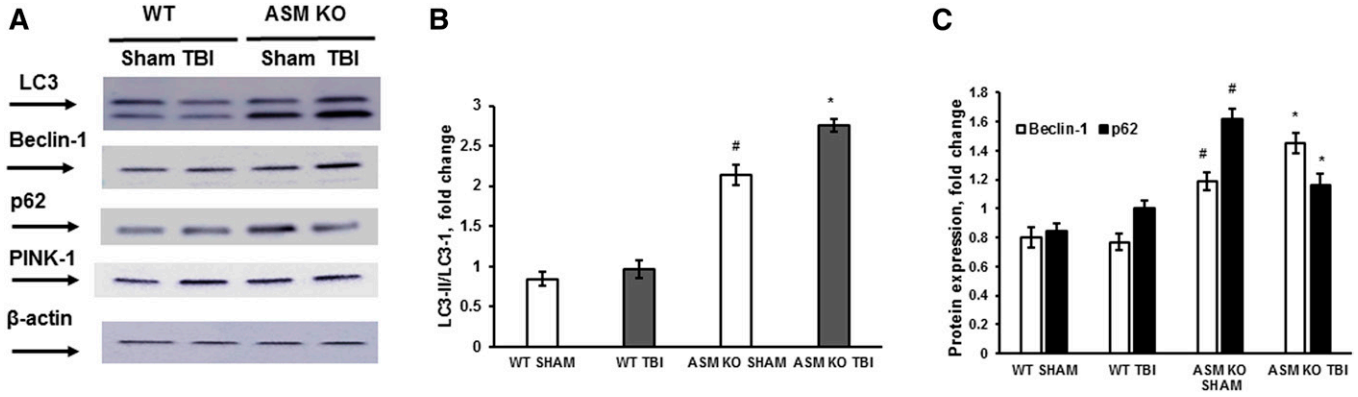

Fig. 4. Elevated autophagy in the ASM-deficient brain is augmented after TBI. Brain tissue samples were prepared from the injured brain of WT and ASM KO mice at 168 h (7 days) post-TBI. Sham-injured animal brain (sham) was used as a control. A: Equal amount of sample (30 μg) was loaded into the lane. The expression of autophagy protein markers was characterized by Western blotting using anti-LC3, anti-Beclin-1, anti-PINK-1, and anti-p62 specific antibodies. To confirm equal loading of samples, the membranes were stripped and probed with anti-β-actin antibody. Representative data are from six independent experiments. Quantification of the LC3-II/LC3-I protein expression ratio (B) and the protein expression of p62 and Beclin-1 (C) using ImageJ software. Data are means ± SE. * $P < 0.05$ (compared with sham); $^{\#}P < 0.05$ (WT versus ASM KO, n = 6).

ASM deficiency is accompanied by an augmented autophagy in the mouse brain. This is in line with a recent study showing that an inhibition of baseline ASM activity was sufficient to initiate autophagy via reducing mTOR signaling in primary lung endothelial cells (63). After CCI insult, the expression ratio of LC3-II/LC3-I and the expression of Beclin-1 were elevated compared with sham, revealing an induction of autophagy during the development of secondary brain injury in the ASM KO mice. The expression of p62 was reduced in the ASM KO mouse brain at 168 h (7 days) post-TBI compared with sham, which is indicative of increased autophagic flux. Similar to WT, there was no change in the expression of PINK-1 in the ASM-deficient brain response to injury, indicating the lack of mitophagy involvement in secondary brain-injury mechanisms. The data suggest that the autophagy was activated in an ASM-deficient brain at the baseline and during the development of secondary brain injury, which could contribute to preservation of mitochondrial function by facilitated removal of damaged organelles.

ASM KO or blocking ASM activity improved behavioral deficits recovery after TBI

To examine the impact of ASM on brain-function recovery after the injury, behavioral deficits were assessed in WT and ASM KO mice after TBI. A standard rotarod test was used, as it has been shown to be effective and reliable in rodent-brain trauma experiments (38). Consistent with previous reports (16, 38), the WT mice had significant impairments in sensorimotor functions, which were gradually recovered up to 59% compared with sham-injured mice at 168 h postinjury (**Fig. 5A**). ASM deficiency significantly improved the sensorimotor function recovery after TBI, revealing the critical role of ASM in the molecular mechanisms underlying behavioral deficits after brain trauma. To investigate whether the ASM activity is necessary for promoting secondary brain injury, a potent inhibitor of ASM activity was used. It has been demonstrated that several bisphosphonate compounds are selective direct inhibitors of ASM activity (64, 65). The most potent of the bisphosphonate derivatives, zoledronic acid (Reclast), a Food and Drug Administration (FDA)-approved drug for the treatment of osteoporosis, exhibited an IC_{50} of 20 nM toward ASM in vitro (64). We have previously shown that Reclast is the most potent inhibitor of ASM activity in primary oligodendrocytes, myelin-forming cells abundant in the brain (24). Brain-function recovery after injury was determined in WT mice treated with Reclast (2 mg/kg) via intraperitoneal injection 1 h after the CCI. Mice exposed to Reclast showed significantly better sensorimotor functions recovery at 48 and 168 h post-TBI (Fig. 5B) compared with vehicle-treated control mice. The data suggest that elevated ASM activity is an important component of the dynamic process propagating secondary brain injury that impacts the recovery of function, and hindering ASM ameliorates sensorimotor impairments after TBI.

To assess the role of ASM in brain cognitive deficits after TBI, we utilized a standard MWM test, which is commonly used for spatial learning and memory testing (39–41). MWM performance as measured by latency to reach the hidden platform was compared between WT and ASM KO mice groups. All experimental animals acquired the MWM learning task, as demonstrated by their ability to reduce their escape latencies following training (**Fig. 6A**). Sham animals (WT and ASM KO) performed significantly better during the MWM task (i.e., shorter latency to reach the goal platform) as compared with the WT-TBI group. The WT injured mice did not improve their performance beyond the second trial day, whereas sham-injured (WT-sham) mice improved their performance throughout the 4 day trial period. Remarkably, the performance of ASM-deficient mice after TBI was significantly better than the WT mice (Fig. 6A). The probe trial consisted of a single 90 s trial, with the platform removed, after the final day of hidden-platform testing (Fig. 6B). There were no differences between sham WT and ASM KO mouse performances in

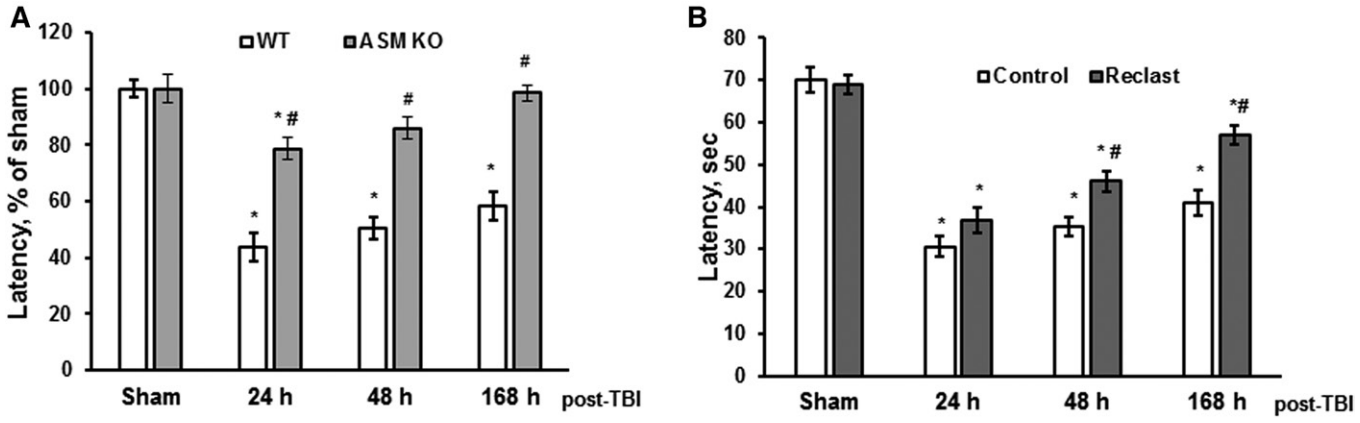

Fig. 5. Hindering ASM improved sensorimotor deficits recovery after brain trauma. Sensorimotor deficits were assessed using a standard rotarod test. Each day for 3 days prior to injury, animals were trained on the rotarod at a speed of 18 rpm in the acceleration mode (0–18 rpm/90 s). Animals were tested with the rotarod apparatus using three trials in session, with a minimum of 5 min resting between trials. Time course of latency changes was determined in WT and ASM KO mice after CCI (A) or in WT mice treated with Reclast (Reclast) compared with vehicle-treated WT mice (control) (B). Data are means ± SE. * $P < 0.05$ (compared with sham or control); # $P < 0.05$ (WT versus ASM KO, n = 16).

MWM tests. Sham animals and the TBI-ASM KO group had significantly better memory retention of the platform location as compared with the WT-TBI group. Together, these studies indicate an essential role of ASM in sensorimotor and cognitive function impairment following TBI.

TBI-triggered ASM activation leads to elevated NLRP3 inflammasome assembly and activity

Brain trauma prompts the release of endogenous mediators acting as danger signals, damage-associated molecular patterns, such as extracellular ATP or heat shock proteins. Their recognition by the innate immune system results in production of inflammatory cytokines, including TNF-α and IL-1β, which activates the adaptive immune response (66). A key component of the brain innate immune response is the NLRP3 inflammasome, an NLR-based multiprotein complex responsible for the activation of caspase-1, leading to processing and secretion of proinflammatory IL-1β and IL-18, which are elevated in human or animal brains following TBI (67). Many cell types in the CNS, including endothelial cells, microglia, astrocytes, and neurons, are capable of assembling the NLRP3 inflammasome,

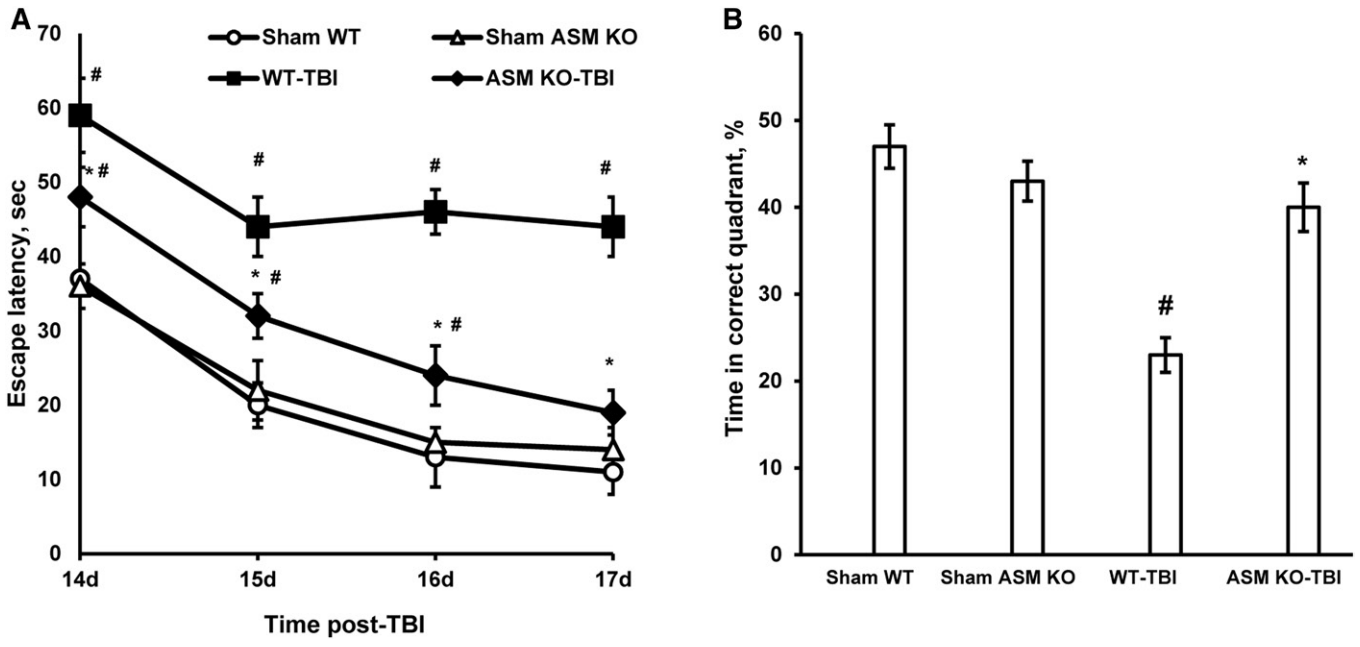

Fig. 6. ASM deficiency improved spatial learning and memory after TBI. Cognitive deficits were assessed using the MWM test in WT and ASM KO mice. A: Spatial learning was assessed in training trials starting at day 14 post-TBI. The mice were exposed to four MWM trials/day, with the hidden-platform location unchanged. Data are means ± SE. * $P < 0.05$ (WT-TBI versus ASM KO-TBI); # $P < 0.05$ (WT-TBI or ASM KO-TBI compared with sham, n = 16). B: On day 18 post-TBI, the platform was removed, and the mice were placed back in the MWM for 90 s. The percent of total time spent in the correct quadrant was recorded as an indicator of spatial memory. Data are means ± SE. * $P < 0.05$ (WT-TBI versus ASM KO-TBI); # $P < 0.05$ (WT-TBI or ASM KO-TBI compared with sham, n = 16).

which is associated with mitochondria via an adaptor protein, MAVS (13). The NLRP3 inflammasome activates the processing of pro-caspase-1, leading to formation of the active caspase-1. Emerging evidence suggests that mitochondrial dysfunction and/or destabilization, including but not limited to elevated ROS production and mitochondrial permeability pore opening, results in activation of the NLRP3 inflammasome. It has been demonstrated that elevated ROS production due to inhibition of the mitochondrial respiratory-chain activity was sufficient to activate the NLRP3 inflammasome (68).

Having demonstrated ASM-dependent inhibition of respiratory-chain activity, we sought to determine whether the ASM-linked mitochondrial dysfunction could be involved in facilitating the neuroinflammatory response to TBI. Following the WT and ASM-deficient mouse exposure to CCI injury, the expression of NLRP3 inflammasome-relevant protein markers was evaluated during the first month post-TBI (**Fig. 7**). In the WT brain, TBI triggered a robust increase in NLRP3 protein expression of about 5-fold at 7 days compared with sham, which was gradually diminished to an approximately 2-fold increase at 28 days (Fig. 7A, B). The expression levels of MAVS were not changed, indicating an abundant availability of the adaptor protein that is required for the maximal activity of the mitochondria-associated NLRP3 inflammasome (not shown). The expression of caspase-1 was increased at 7 days (3.2-fold), peaking at 14 days (4-fold), and remaining up to a 3-fold increase at 21 and 28 days compared with sham (Fig. 7A, C). The increases in caspase-1 protein expression suggest that TBI elicited enhancement of NLRP3 inflammasome activity during the first month post-TBI. In the ASM-deficient mouse brain, TBI triggered an increase in NLRP3 protein expression up to 2.2-fold at 7 days compared with sham that was gradually subsided to about a 1.3-fold increase at 28 days (Fig. 7A, B). The caspase-1 protein expression was increased up to 2.5-fold at 7 days, peaking at 14 days (3-fold) and gradually subsiding to 1.8-fold at 28 days compared with sham (Fig. 7A, C). These studies indicate that TBI-triggered assembly and activation of the NLRP3 inflammasome were significantly attenuated in the ASM-deficient mouse brain.

To investigate whether the ASM activity is necessary for TBI-induced activation of the NLRP3 inflammasome, WT mice were treated with a potent inhibitor of ASM activity, Reclast (2 mg/kg, ip), 1 h after the CCI. The TBI-triggered elevation of NLRP3 protein expression in the brain of WT mice treated with Reclast was about 39% lower at 7 days and 34% lower at 14 days post-TBI compared with WT mice (Fig. 7A, B). Reclast treatment significantly decreased the TBI-induced caspase-1 expression at 14 days post-TBI, but did not have an impact at 7, 21, or 28 days post-TBI (Fig. 7A, C). The data suggest that TBI-triggered ASM activation is an important determinant of the neuroinflammatory cascade directing assembly and activity of the NLRP3 inflammasome after brain trauma.

ASM deficiency alleviated early stages of reactive astrogliosis after TBI

TBI sets in motion multifaceted events in which harmful mechanical forces disrupt CNS homeostasis and triggers diverse multicellular responses that evolve over time and can lead either to neural repair or secondary cellular injury. Astrocytes, the most prevalent glial cells in the brain,

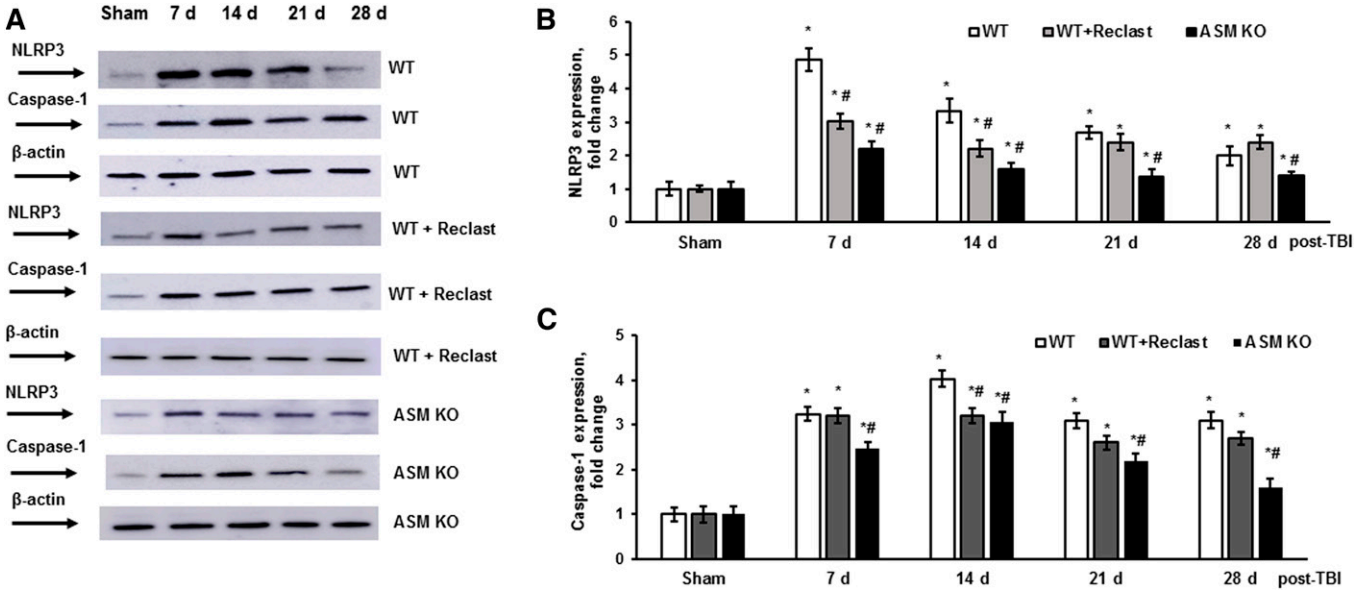

Fig. 7. TBI-triggered NLRP3 inflammasome activation is attenuated in the ASM-deficient brain. Brain tissue samples were prepared from the injured brain of WT, ASM KO, and WT mice treated with Reclast (2 mg/kg, ip). Sham-injured animal brain (sham) was used as a control. A: Equal amount of sample (30 μg) was loaded into the lane. The expression of protein markers of the NLRP3 inflammasome were characterized by Western blotting. To confirm equal loading of samples, the membranes were stripped and probed with anti-β-actin antibody. Representative data are from six independent experiments. Quantification of the normalized NLRP3 protein expression (B) and the normalized protein expression of caspase-1 (C) using ImageJ software. Data are means ± SE. * $P < 0.05$ (n = 6 compared with sham); $^{\#}P < 0.05$ (n = 6, WT versus WT+ Reclast or ASM KO).

are active participants in a variety of CNS functions such as synaptogenesis, neuronal transmission, and synaptic plasticity. Astrocytes sense changes in neuronal activity and exert homeostatic mechanisms fundamental for maintaining neural circuit function, including buffering neurotransmitters, modulating extracellular osmolarity, and controlling neurovascular coupling. In response to brain injury, astrocytes undergo progressive changes of gene expression, morphology, and function that are referred to as reactive astrogliosis (69). Upon injury, reactive astrocytes are characterized by their hypertrophy and overexpression of their canonical markers, including the GFAP and other intermediate filaments, vimentin, and nestin. Reactive astrocytes also contribute to the release of proinflammatory and antiinflammatory cytokines, such as transforming growth factor-β, TNF-α, IFN-γ, IL-1, and IL-6 that modulate inflammation and secondary-injury mechanisms. To elucidate the role of ASM in TBI-induced reactive astrogliosis, the expression of GFAP was determined in the injured brain of WT and ASM-deficient mice during the first month after TBI (**Fig. 8**). The expression of an Aldh1l1 protein was used as a pan-astrocyte marker (70). Consistent with previous reports (71, 72), GFAP expression was significantly enhanced at 7 days up to 2.5-fold, which was followed by further increases up to 3-fold at 14 days and up to 3.6-fold at 21 and 28 days, compared with sham. There were no changes in the expression of Aldh1l1 protein after TBI, indicating a lack of increase in astrocyte proliferation. In the ASM-deficient brain, the GFAP expression was elevated up to 1.9-fold at 7 days post-TBI, compared with sham; however, that was a 39% lower increase in GFAP level compared with WT (Fig. 8). There were no significant differences between dynamics of TBI-induced GFAP expression in WT and ASM-deficient mice at later time points during the first month post-TBI. Of note, there were no changes in the expression of Aldh1l1 protein in the WT or ASM-deficient brain after TBI, supporting the notion that augmented GFAP expression reflects the activation of astrocytes, not proliferation. To investigate whether the ASM activity is necessary for TBI-induced reactive astrogliosis, WT mice were treated with a potent inhibitor of ASM activity, Reclast (2 mg/kg ip), 1 h after the CCI. Reclast treatment significantly lowered the TBI-induced GFAP expression at 7 days post-TBI, but did not have any impact at later time points. The data suggest that TBI-induced activation of ASM is an essential factor promoting astrocyte activation at the initial stages of the reactive astrogliosis progression during the brain response to trauma.

DISCUSSION

Our studies establish a fundamental role of ASM in the multifaceted mechanisms governing secondary brain injury after TBI. The data indicate that TBI-triggered activation of ASM and upregulation of mitochondrial sphingosine result in mitochondrial respiratory-chain malfunction, leading to an enhanced assembly and activity of the NLRP3 inflammasome, a pivotal factor promoting the neuroinflammatory response to brain injury. The results of our studies provide further support for the emerging role of ASM in repressing the cell-maintenance and quality-control mechanism, autophagy, which is essential for the neural cell survival after the injury. Thus, ASM KO rescued mitochondrial defect, augmented the autophagic flux, downregulated the NLRP3 inflammasome, and improved the brain-function recovery after TBI. Importantly, ASM deficiency did not have a major impact on the progression of astrogliosis, a brain defense mechanism wherein activated astrocytes minimize spread of the neuroinflammation and

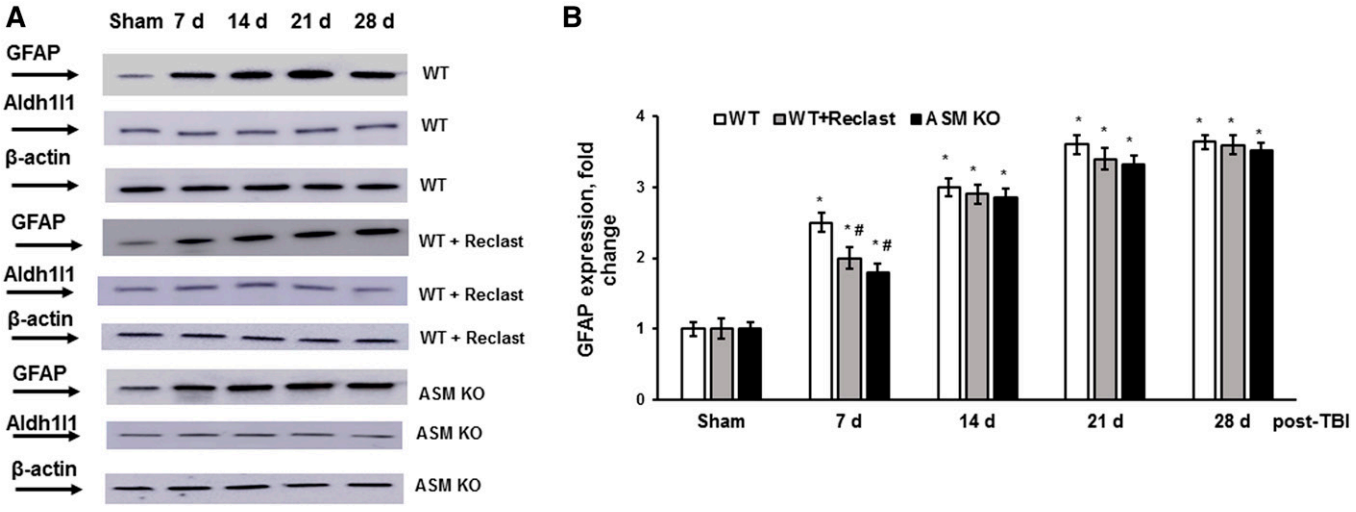

Fig. 8. ASM deficiency impacted the early reactive astrogliosis after brain trauma. Brain tissue samples were prepared from the injured brain cortex of WT, ASM KO, and WT mice treated with Reclast (2 mg/kg, ip). Sham-injured animal brain (sham) was used as a control. A: Equal amount of sample (30 μg) was loaded into the lane. The expression of panastrocyte marker Aldh1l1 and reactive astrocyte marker GFAP were determined by Western blotting. To confirm equal loading of samples, the membranes were stripped and probed with anti-β-actin antibody. Representative data are from six independent experiments. B: Quantification of the normalized GFAP protein expression using ImageJ software. Data are means ± SE. * $P < 0.05$ (n = 6 compared with sham); # $P < 0.05$ (n = 6, WT versus ASM KO).

further tissue repair and regeneration in response to TBI. Our novel findings reveal that ASM, a critical player promoting secondary brain injury and neuroinflammation, is uniquely positioned to be a promising target for the development of effective pharmacological treatment of patients with TBI.

These studies expand the experimental support for the central role of brain sphingolipidome disturbance in the development of secondary brain injury after trauma. TBI has been shown to instigate a substantial deregulation of cerebral sphingolipid metabolism, manifested by increases in SM species and sphingosine concurrently with upregulation of intermediates of de novo sphingolipid biosynthesis (16). Proteomic analysis showed a lack of changes in the expression level of 40 genes involved in sphingolipid metabolism, suggesting that secondary TBI proceeds through posttranslational mechanisms of enzyme modulation. Investigation of intracellular sites of sphingolipid changes revealed a robust elevation of sphingosine in mitochondria that resulted in the reduced activity of the mitochondrial respiratory-chain enzyme COX. The increased mitochondrial sphingosine content has been shown to be partly due to the TBI-induced disruption of the sphingosine-metabolizing enzyme activity at the mitochondrial level. Thus, TBI triggered an activation of the mitochondrial NCDase, generating sphingosine that was exacerbated with its reduced utilization by mitochondrial sphingosine kinase 2 (16). Our current studies identify the activation of lysosomal ASM as an important source of sphingosine contributing to mitochondrial sphingosine accumulation in the injured brain. (Figs. 1, 2).

Activation of ASM could be the interplay of several mechanisms involved in the development of secondary brain damage, such as proinflammatory cytokines, oxidative stress, glutamate oxidative toxicity, and disintegration of extracellular matrix (ECM). First, ASM activation is known to be triggered by proinflammatory cytokines, such as TNF-α, IL-1β, and IL-6, as well as by platelet-activating factor, a lipid mediator of inflammation, leading to apoptotic cell death in various cell types (73, 74). It has been demonstrated that TNF-α-induced apoptosis was mediated by ASM and attenuated by the inhibitors of the ASM activity in dopaminergic neurons (27). In glial cells, activation of ASM was necessary for the formation and release of IL-1β-containing microparticles in response to extracellular ATP binding to ionotropic ATP receptor $P2X_7$ (75). In TBI, activation of the receptor could occur at the lesion site by ATP leaking from the neighboring injured cells or, distantly from the lesion, through propagation of ATP-mediated Ca^{2+} wave among astrocytes. It appears that astrocytic Ca^{2+} waves underlie the phenomenon of spreading depression in the brain, a pathological suppression of cortical neuronal excitability implicated in the propagation of brain injury in TBI (76). Of note, systemic administration of an antagonist of ATP-sensitive receptor $P2X_7$ reduced anatomical spinal cord damage and improved motor recovery from traumatic spinal cord injury (77).

Second, oxidative stress could trigger intracellular Ca^{2+}-dependent lysosome trafficking and enhance ASM activity, leading to ASM translocation to the plasma membrane and formation of ceramide-enriched domains accelerating apoptotic signal transduction (28). In the injured cells, extracellular Ca^{2+} influx induces exocytosis of lysosomes and association of ASM with the plasma membrane, where the enzyme triggers ceramide-mediated invagination of the damaged plasma membrane to facilitate endocytosis and damage repair (26).

Third, recently, ASM has been implicated as a critical determinant in a newly discovered form of programmed cell death, ferroptosis, that was induced by excessive extracellular glutamate, a key factor in secondary brain injury (24). In oligodendrocytes, the myelin-forming cells in the CNS, glutamate-induced decline of intracellular GSH, resulted in a selective increase of ASM, not NSM, activity leading to sphingosine-mediated mitochondrial dysfunction, elevated mitochondrial ROS, oxidative lipid damage, and necrotic cell death. ASM inhibitors (Reclast or desipramine) or Smpd1 gene ablation preserved mitochondrial function, reduced ROS generation and oxidative lipid damage, and augmented oligodendrocyte survival in response to glutamate.

Fourth, emerging data suggest that disturbed interaction of integrin receptors with ECM plays a critical role in the brain tissue injury. Integrin receptor engagement with ECM initiates an assembly of an adhesion-dependent signaling scaffold containing a number of adaptor proteins and kinases, leading to activation of signaling pathways aimed to prevent apoptosis, which has been demonstrated in the TBI-injured human brain (11). The disruption of the $\alpha_v\beta_3$ integrin receptor signaling by RNA interference or a specific inhibitor of integrin activity (RGD peptide) resulted in activation of ASM and ceramide accumulation, leading to apoptosis in oligodendrocytes (44) and endothelial cells (78).

Our studies extend the experimental evidence of a prominent role of the ASM/sphingosine axis in perturbing mitochondrial function that underlies the brain-function impairments after trauma. Consistent with a previous report (16), TBI-triggered accumulation of sphingosine in cerebral mitochondria resulted in an attenuated COX activity and an elevated oxidative proteins modification (Fig. 3). Importantly, TBI-induced mitochondrial abnormalities were rescued in the ASM-deficient brain. Moreover, ASM KO or blocking ASM activity with Reclast significantly improved sensorimotor and cognitive deficit recovery after TBI (Figs. 5, 6). The results of these studies suggest that ASM-dependent mitochondrial dysfunction is crucial for propagating the secondary brain injury, and hindering ASM could be a promising strategy for improving brain-function recovery after TBI.

These studies provide further support for the importance of the innate immune-response mechanisms in secondary brain injury and highlight a novel role of ASM as a facilitator of assembly and function of the NLRP3 inflammasome. In acute CNS injury models, a spectrum of inflammatory events have been reported, including activation and recruitment of inflammatory cells, increased gene expression, and protein levels of proinflammatory cytokines

that could lead to both detrimental and reparative processes. An increased production of IL-1β and IL-18 has been widely implicated in the pathophysiology of spinal cord injury, stroke, and TBI, but the mechanism of their generation involving an activation of the NLRP3 inflammasome has been recently uncovered (15). An augmented mRNA and protein expression of NLRP3 as well as a rise of caspase-1 protein expression were described in animal TBI models during the first week postinjury (14, 79). Inhibiting the NLRP3 inflammasome activation in CNS appears to serve as a potential and effective pathway for the attenuation of the secondary brain injury. Thus, MCC950, a potent inhibitor of NLRP3 inflammasome activation, was reported to alleviate the severity of acute brain injury; however, its impact on chronic neuroinflammation was not investigated (80). Our studies demonstrate a novel mechanism of NLRP3 inflammasome activation that involves ASM/sphingosine-dependent mitochondrial dysfunction, leading to chronic upregulation of NLRP3 and caspase-1 protein expression after TBI (Fig. 7). Therefore, the chronic activation of the NLRP3 inflammasome after TBI was attenuated in ASM-deficient mice and in WT mice treated with Reclast, a potent inhibitor of ASM activity (24, 65). One can only speculate that a sustained ASM activation following TBI is a part of a vicious cycle of sphingosine-mediated mitochondrial dysfunction and neuroinflammation. It is conceivable that the initial TBI-induced oxidative stress results in reduced GSH, leading to ASM activation (24) and accumulation of mitochondrial sphingosine that prompts mitochondrial dysfunction, ROS production, and activation of the NLRP3 inflammasome. Rising proinflammatory cytokines could activate ASM (73), which results in increased mitochondrial sphingosine, leading to enhanced mitochondrial ROS, promoting neuroinflammation and chronic brain impairment.

Our studies provide further support for the notion that mitochondrial respiratory-chain dysfunction is a potent trigger for the NLRP3 inflammasome activation along with other known mitochondrion-associated signals, such as mitochondrial DNA release and externalized cardiolipin (81). However, the contribution of a mitochondria-independent mechanism of ASM and/or sphingosine involvement in NLRP3 inflammasome activation cannot be ruled out. Thus, sphingosine has been shown to stimulate permeabilization of lysosomes acting as lysosomotropic agent (82). Conversely, destabilization of lysosomes using a lysosomotropic agent (Leu-Leu-OMe) resulted in upregulation of the NLRP3 inflammasome, leading to caspase-1-mediated cells death, pyroptosis (83).

Emerging evidence supports a fundamental function of ASM/sphingosine in the regulation of lysosome homeostasis. Recently, it has been demonstrated that a baseline ASM activity is required for mTOR signaling and autophagy inhibition (63). Blocking ASM activity with imipramine or knocking down ASM expression with siRNA markedly reduced mTOR phosphorylation, instigating the modification of transcription factor EB and activation of autophagy. In line with these studies, our data show an augmented autophagic flux in a baseline ASM-deficient mouse brain, supporting the ASM/sphingosine role in controlling lysosome functions (Fig. 4). TBI elicited further activation of autophagy in the brain of ASM KO mice that is consistent with ASM/sphingosine acting as an inhibitor of autophagy (63). Although the accurate role of autophagy in TBI remains to be established, many studies show that autophagy participates in the secondary mechanisms of brain injury after TBI and that activation of autophagy could provide neuroprotection and ameliorate brain impairments (59).

There is increasing recognition that the potential beneficial or sometimes harmful effects of cellular responses to TBI, such as activation of autophagy or reactive astrogliosis, are determined by a multitude of specific signaling events defined by the nature and severity of the CNS insult. Mounting data suggest that reactive astrocytes perform essential functions in the regulation and restriction of neuroinflammation and the preservation of the tissue post-TBI. Experimental evidence supports the notion that reactive astrocytes are instrumental in preserving injured but salvageable tissue (71). In response to brain injury or inflammation, reactive astrocytes form scar borders that segregate the damaged and inflamed tissue from potentially viable neural tissue. These scar borders comprise almost entirely newly proliferated astrocytes, which exhibit barrier functions regulating the expansion of tissue injury, inflammation, and coordinating the wound repair process (72). Thus, genetic ablation of reactive astrocytes responding to TBI resulted in a greatly intensified neuroinflammatory response with pronounced neurodegeneration (84). Although astrogliosis is recognized as a defense mechanism to minimize and repair the initial damage, it could lead to detrimental effects. In spinal cord injury, reactive astrogliosis resulted in the formation of irreversible glial scarring that acted as a barrier to recovery due to the overexpression of chondroitin sulfate proteoglycans, potent inhibitors of neural repair and regeneration (85). The results of our studies demonstrate that ASM is necessary for the initial stages of reactive astrogliosis in the injured brain and does not play a major role in later stages of the progression of reactive astrogliosis.

Considerable research effort aimed to develop neuroprotective treatments for TBI suggested many promising pharmacologic agents showing efficacy in preclinical studies. However, more than 30 phase III prospective clinical trials have failed to show significance for their primary end point (86). These trials mostly targeted single factors proposed to mediate the secondary brain injury, whereas the complexity and diversity of secondary injury mechanisms led to calls to target multiple delayed injury pathways (87). Given the multifactorial nature of the secondary injury processes after brain trauma, it is highly unlikely that targeting any single factor will result in significant improvement of the outcome after TBI in human injury. In contrast, simultaneous targeting of several mechanisms propagating the injury using multipotential drugs may maximize the likelihood of developing an effective therapeutic intervention for TBI patients. The results of our studies demonstrate that ASM is critically involved in several dynamic processes implicated in progression of the brain injury after trauma,

including mitochondrial dysfunction, neuroinflammation, and reactive astrogliosis. It appears that ASM could be a promising target for the development of a successful multipotential drug for TBI treatment that may involve repurposing of an FDA-approved inhibitor of ASM activity, Reclast.

These studies provide experimental evidence that TBI-triggered activation of ASM results in mitochondrial impairment-instigated elevation of NLRP3 inflammasome activity promoting brain-function deficits and highlight a fundamental role of sphingolipid-metabolizing enzymes in the neuroinflammation processes following brain trauma.

The authors thank Alexander S. Novgorodov for help with preparation of the manuscript. The Lipidomics Core Facility at the Medical University of South Carolina was supported in part by National Institutes of Health Grant P30 GM103339.

REFERENCES

1. Brooks, J. C., D. J. Strauss, R. M. Shavelle, D. R. Paculdo, F. M. Hammond, and C. L. Harrison-Felix. 2013. Long-term disability and survival in traumatic brain injury: results from the National Institute on Disability and Rehabilitation Research Model Systems. *Arch. Phys. Med. Rehabil.* **94:** 2203–2209.
2. Maas, A. I., N. Stocchetti, and R. Bullock. 2008. Moderate and severe traumatic brain injury in adults. *Lancet Neurol.* **7:** 728–741.
3. Werner, C., and K. Engelhard. 2007. Pathophysiology of traumatic brain injury. *Br. J. Anaesth.* **99:** 4–9.
4. Guerriero, R. M., C. C. Giza, and A. Rotenberg. 2015. Glutamate and GABA imbalance following traumatic brain injury. *Curr. Neurol. Neurosci. Rep.* **15:** 27.
5. Xiong, Y., Y. Zhang, A. Mahmood, and M. Chopp. 2015. Investigational agents for treatment of traumatic brain injury. *Expert Opin. Investig. Drugs.* **24:** 743–760.
6. Faden, A. I., J. Wu, B. A. Stoica, and D. J. Loane. 2016. Progressive inflammation-mediated neurodegeneration after traumatic brain or spinal cord injury. *Br. J. Pharmacol.* **173:** 681–691.
7. Omalu, B., J. Bailes, R. L. Hamilton, M. I. Kamboh, J. Hammers, M. Case, and R. Fitzsimmons. 2011. Emerging histomorphologic phenotypes of chronic traumatic encephalopathy in American athletes. *Neurosurgery.* **69:** 173–183, discussion 183.
8. Scott, G., A. F. Ramlackhansingh, P. Edison, P. Hellyer, J. Cole, M. Veronese, R. Leech, R. J. Greenwood, F. E. Turkheimer, S. M. Gentleman, et al. 2016. Amyloid pathology and axonal injury after brain trauma. *Neurology.* **86:** 821–828.
9. Cheng, G., R. H. Kong, L. M. Zhang, and J. N. Zhang. 2012. Mitochondria in traumatic brain injury and mitochondrial-targeted multipotential therapeutic strategies. *Br. J. Pharmacol.* **167:** 699–719.
10. Bittigau, P., M. Sifringer, D. Pohl, D. Stadthaus, M. Ishimaru, H. Shimizu, M. Ikeda, D. Lang, A. Speer, J. W. Olney, et al. 1999. Apoptotic neurodegeneration following trauma is markedly enhanced in the immature brain. *Ann. Neurol.* **45:** 724–735.
11. Ng, I., T. T. Yeo, W. Y. Tang, R. Soong, P. Y. Ng, and D. R. Smith. 2000. Apoptosis occurs after cerebral contusions in humans. *Neurosurgery.* **46:** 949–956.
12. Maiuri, M. C., E. Zalckvar, A. Kimchi, and G. Kroemer. 2007. Self-eating and self-killing: crosstalk between autophagy and apoptosis. *Nat. Rev. Mol. Cell Biol.* **8:** 741–752.
13. Subramanian, N., K. Natarajan, M. R. Clatworthy, Z. Wang, and R. N. Germain. 2013. The adaptor MAVS promotes NLRP3 mitochondrial localization and inflammasome activation. *Cell.* **153:** 348–361.
14. Liu, H. D., W. Li, Z. R. Chen, Y. C. Hu, D. D. Zhang, W. Shen, M. L. Zhou, L. Zhu, and C. H. Hang. 2013. Expression of the NLRP3 inflammasome in cerebral cortex after traumatic brain injury in a rat model. *Neurochem. Res.* **38:** 2072–2083.
15. de Rivero Vaccari, J. P., W. D. Dietrich, and R. W. Keane. 2014. Activation and regulation of cellular inflammasomes: gaps in our knowledge for central nervous system injury. *J. Cereb. Blood Flow Metab.* **34:** 369–375.
16. Novgorodov, S. A., C. L. Riley, J. Yu, K. T. Borg, Y. A. Hannun, R. L. Proia, M. S. Kindy, and T. I. Gudz. 2014. Essential roles of neutral ceramidase and sphingosine in mitochondrial dysfunction due to traumatic brain injury. *J. Biol. Chem.* **289:** 13142–13154.
17. Hannun, Y. A., and L. M. Obeid. 2008. Principles of bioactive lipid signalling: lessons from sphingolipids. *Nat. Rev. Mol. Cell Biol.* **9:** 139–150.
18. Gupta, S., M. R. Maurya, A. H. Merrill, Jr., C. K. Glass, and S. Subramaniam. 2011. Integration of lipidomics and transcriptomics data towards a systems biology model of sphingolipid metabolism. *BMC Syst. Biol.* **5:** 26.
19. Henry, B., R. Ziobro, K. A. Becker, R. Kolesnick, and E. Gulbins. 2013. Acid sphingomyelinase. *Handb. Exp. Pharmacol.* 77–88.
20. Tidhar, R., and A. H. Futerman. 2013. The complexity of sphingolipid biosynthesis in the endoplasmic reticulum. *Biochim. Biophys. Acta.* **1833:** 2511–2518.
21. Kitatani, K., J. Idkowiak-Baldys, and Y. A. Hannun. 2008. The sphingolipid salvage pathway in ceramide metabolism and signaling. *Cell. Signal.* **20:** 1010–1018.
22. Stiban, J., L. Caputo, and M. Colombini. 2008. Ceramide synthesis in the endoplasmic reticulum can permeabilize mitochondria to proapoptotic proteins. *J. Lipid Res.* **49:** 625–634.
23. Chatelut, M., M. Leruth, K. Harzer, A. Dagan, S. Marchesini, S. Gatt, R. Salvayre, P. Courtoy, and T. Levade. 1998. Natural ceramide is unable to escape the lysosome, in contrast to a fluorescent analogue. *FEBS Lett.* **426:** 102–106.
24. Novgorodov, S. A., J. R. Voltin, M. A. Gooz, L. Li, J. J. Lemasters, and T. I. Gudz. 2018. Acid sphingomyelinase promotes mitochondrial dysfunction due to glutamate-induced regulated necrosis. *J. Lipid Res.* **59:** 312–329.
25. Stancevic, B., and R. Kolesnick. 2010. Ceramide-rich platforms in transmembrane signaling. *FEBS Lett.* **584:** 1728–1740.
26. Tam, C., V. Idone, C. Devlin, M. C. Fernandes, A. Flannery, X. He, E. Schuchman, I. Tabas, and N. W. Andrews. 2010. Exocytosis of acid sphingomyelinase by wounded cells promotes endocytosis and plasma membrane repair. *J. Cell Biol.* **189:** 1027–1038.
27. Martinez, T. N., X. Chen, S. Bandyopadhyay, A. H. Merrill, and M. G. Tansey. 2012. Ceramide sphingolipid signaling mediates tumor necrosis factor (TNF)-dependent toxicity via caspase signaling in dopaminergic neurons. *Mol. Neurodegener.* **7:** 45.
28. Li, X., E. Gulbins, and Y. Zhang. 2012. Oxidative stress triggers Ca-dependent lysosome trafficking and activation of acid sphingomyelinase. *Cell. Physiol. Biochem.* **30:** 815–826.
29. Beckmann, N., D. Sharma, E. Gulbins, K. A. Becker, and B. Edelmann. 2014. Inhibition of acid sphingomyelinase by tricyclic antidepressants and analogons. *Front. Physiol.* **5:** 331.
30. Gulbins, E., M. Palmada, M. Reichel, A. Luth, C. Bohmer, D. Amato, C. P. Muller, C. H. Tischbirek, T. W. Groemer, G. Tabatabai, et al. 2013. Acid sphingomyelinase-ceramide system mediates effects of antidepressant drugs. *Nat. Med.* **19:** 934–938.
31. Gulbins, A., F. Schumacher, K. A. Becker, B. Wilker, M. Soddemann, F. Boldrin, C. P. Muller, M. J. Edwards, M. Goodman, C. C. Caldwell, et al. 2018. Antidepressants regulate autophagy by targeting acid sphingomyelinase. *Mol. Psychiatry.* **23:** 2251.
32. Lee, J. K., H. K. Jin, M. H. Park, B. R. Kim, P. H. Lee, H. Nakauchi, J. E. Carter, X. He, E. H. Schuchman, and J. S. Bae. 2014. Acid sphingomyelinase modulates the autophagic process by controlling lysosomal biogenesis in Alzheimer's disease. *J. Exp. Med.* **211:** 1551–1570.
33. Horinouchi, K., S. Erlich, D. P. Perl, K. Ferlinz, C. L. Bisgaier, K. Sandhoff, R. J. Desnick, C. L. Stewart, and E. H. Schuchman. 1995. Acid sphingomyelinase deficient mice: a model of types A and B Niemann-Pick disease. *Nat. Genet.* **10:** 288–293.
34. Lozano, J., A. Morales, A. Cremesti, Z. Fuks, J. L. Tilly, E. Schuchman, E. Gulbins, and R. Kolesnick. 2001. Niemann-Pick disease versus acid sphingomyelinase deficiency. *Cell Death Differ.* **8:** 100–103.
35. Saatman, K. E., K. J. Feeko, R. L. Pape, and R. Raghupathi. 2006. Differential behavioral and histopathological responses to graded cortical impact injury in mice. *J. Neurotrauma.* **23:** 1241–1253.
36. Washington, P. M., P. A. Forcelli, T. Wilkins, D. N. Zapple, M. Parsadanian, and M. P. Burns. 2012. The effect of injury severity on behavior: a phenotypic study of cognitive and emotional deficits after mild, moderate, and severe controlled cortical impact injury in mice. *J. Neurotrauma.* **29:** 2283–2296.
37. Hamm, R. J., B. R. Pike, D. M. O'Dell, B. G. Lyeth, and L. W. Jenkins. 1994. The rotarod test: an evaluation of its effectiveness in assessing motor deficits following traumatic brain injury. *J. Neurotrauma.* **11:** 187–196.

38. Fujimoto, S. T., L. Longhi, K. E. Saatman, V. Conte, N. Stocchetti, and T. K. McIntosh. 2004. Motor and cognitive function evaluation following experimental traumatic brain injury. *Neurosci. Biobehav. Rev.* **28:** 365–378. [Erratum. 2005. *Neurosci. Biobehav. Rev.* 28:877.]
39. Morris, R. 1984. Developments of a water-maze procedure for studying spatial learning in the rat. *J. Neurosci. Methods.* **11:** 47–60.
40. Hamm, R. J., C. E. Dixon, D. M. Gbadebo, A. K. Singha, L. W. Jenkins, B. G. Lyeth, and R. L. Hayes. 1992. Cognitive deficits following traumatic brain injury produced by controlled cortical impact. *J. Neurotrauma.* **9:** 11–20.
41. Vorhees, C. V., and M. T. Williams. 2006. Morris water maze: procedures for assessing spatial and related forms of learning and memory. *Nat. Protoc.* **1:** 848–858.
42. Yu, J., S. A. Novgorodov, D. Chudakova, H. Zhu, A. Bielawska, J. Bielawski, L. M. Obeid, M. S. Kindy, and T. I. Gudz. 2007. JNK3 signaling pathway activates ceramide synthase leading to mitochondrial dysfunction. *J. Biol. Chem.* **282:** 25940–25949.
43. Novgorodov, S. A., D. A. Chudakova, B. W. Wheeler, J. Bielawski, M. S. Kindy, L. M. Obeid, and T. I. Gudz. 2011. Developmentally regulated ceramide synthase 6 increases mitochondrial Ca2+ loading capacity and promotes apoptosis. *J. Biol. Chem.* **286:** 4644–4658.
44. Chudakova, D. A., Y. H. Zeidan, B. W. Wheeler, J. Yu, S. A. Novgorodov, M. S. Kindy, Y. A. Hannun, and T. I. Gudz. 2008. Integrin-associated Lyn kinase promotes cell survival by suppressing acid sphingomyelinase activity. *J. Biol. Chem.* **283:** 28806–28816.
45. Novgorodov, A. S., M. El-Alwani, J. Bielawski, L. M. Obeid, and T. I. Gudz. 2007. Activation of sphingosine-1-phosphate receptor S1P5 inhibits oligodendrocyte progenitor migration. *FASEB J.* **21:** 1503–1514.
46. Novgorodov, S. A., C. L. Riley, J. A. Keffler, J. Yu, M. S. Kindy, W. B. Macklin, D. B. Lombard, and T. I. Gudz. 2016. SIRT3 deacetylates ceramide synthases: implications for mitochondrial dysfunction and brain injury. *J. Biol. Chem.* **291:** 1957–1973.
47. Clarke, C. J., B. X. Wu, and Y. A. Hannun. 2011. The neutral sphingomyelinase family: identifying biochemical connections. *Adv. Enzyme Regul.* **51:** 51–58.
48. Jenkins, R. W., J. Idkowiak-Baldys, F. Simbari, D. Canals, P. Roddy, C. D. Riner, C. J. Clarke, and Y. A. Hannun. 2011. A novel mechanism of lysosomal acid sphingomyelinase maturation: requirement for carboxyl-terminal proteolytic processing. *J. Biol. Chem.* **286:** 3777–3788.
49. Tani, M., M. Ito, and Y. Igarashi. 2007. Ceramide/sphingosine/sphingosine 1-phosphate metabolism on the cell surface and in the extracellular space. *Cell. Signal.* **19:** 229–237.
50. Morales, D. M., N. Marklund, D. Lebold, H. J. Thompson, A. Pitkanen, W. L. Maxwell, L. Longhi, H. Laurer, M. Maegele, E. Neugebauer, et al. 2005. Experimental models of traumatic brain injury: do we really need to build a better mousetrap? *Neuroscience.* **136:** 971–989.
51. Onyszchuk, G., B. Al-Hafez, Y. Y. He, M. Bilgen, N. E. Berman, and W. M. Brooks. 2007. A mouse model of sensorimotor controlled cortical impact: characterization using longitudinal magnetic resonance imaging, behavioral assessments and histology. *J. Neurosci. Methods.* **160:** 187–196.
52. Zigdon, H., A. Kogot-Levin, J. W. Park, R. Goldschmidt, S. Kelly, A. H. Merrill, Jr., A. Scherz, Y. Pewzner-Jung, A. Saada, and A. H. Futerman. 2013. Ablation of ceramide synthase 2 causes chronic oxidative stress due to disruption of the mitochondrial respiratory chain. *J. Biol. Chem.* **288:** 4947–4956.
53. Zoccarato, F., L. Cavallini, and A. Alexandre. 2009. Succinate is the controller of O2-/H2O2 release at mitochondrial complex I: negative modulation by malate, positive by cyanide. *J. Bioenerg. Biomembr.* **41:** 387–393.
54. Rodríguez-Rodríguez, A., J. J. Egea-Guerrero, F. Murillo-Cabezas, and A. Carrillo-Vico. 2014. Oxidative stress in traumatic brain injury. *Curr. Med. Chem.* **21:** 1201–1211.
55. Bayir, H., V. E. Kagan, R. S. Clark, K. Janesko-Feldman, R. Rafikov, Z. Huang, X. Zhang, V. Vagni, T. R. Billiar, and P. M. Kochanek. 2007. Neuronal NOS-mediated nitration and inactivation of manganese superoxide dismutase in brain after experimental and human brain injury. *J. Neurochem.* **101:** 168–181.
56. Scheff, S. W., D. A. Price, R. R. Hicks, S. A. Baldwin, S. Robinson, and C. Brackney. 2005. Synaptogenesis in the hippocampal CA1 field following traumatic brain injury. *J. Neurotrauma.* **22:** 719–732.
57. Ansari, M. A., K. N. Roberts, and S. W. Scheff. 2008. Oxidative stress and modification of synaptic proteins in hippocampus after traumatic brain injury. *Free Radic. Biol. Med.* **45:** 443–452.
58. Narendra, D. P., and R. J. Youle. 2011. Targeting mitochondrial dysfunction: role for PINK1 and Parkin in mitochondrial quality control. *Antioxid. Redox Signal.* **14:** 1929–1938.
59. Zhang, L., and H. Wang. 2018. Autophagy in traumatic brain injury: a new target for therapeutic intervention. *Front. Mol. Neurosci.* **11:** 190.
60. Luo, C. L., B. X. Li, Q. Q. Li, X. P. Chen, Y. X. Sun, H. J. Bao, D. K. Dai, Y. W. Shen, H. F. Xu, H. Ni, et al. 2011. Autophagy is involved in traumatic brain injury-induced cell death and contributes to functional outcome deficits in mice. *Neuroscience.* **184:** 54–63.
61. Erlich, S., A. Alexandrovich, E. Shohami, and R. Pinkas-Kramarski. 2007. Rapamycin is a neuroprotective treatment for traumatic brain injury. *Neurobiol. Dis.* **26:** 86–93.
62. Heras-Sandoval, D., J. M. Perez-Rojas, J. Hernandez-Damian, and J. Pedraza-Chaverri. 2014. The role of PI3K/AKT/mTOR pathway in the modulation of autophagy and the clearance of protein aggregates in neurodegeneration. *Cell. Signal.* **26:** 2694–2701.
63. Justice, M. J., I. Bronova, K. S. Schweitzer, C. Poirier, J. S. Blum, E. V. Berdyshev, and I. Petrache. 2018. Inhibition of acid sphingomyelinase disrupts LYNUS signaling and triggers autophagy. *J. Lipid Res.* **59:** 596–606.
64. Roth, A. G., D. Drescher, Y. Yang, S. Redmer, S. Uhlig, and C. Arenz. 2009. Potent and selective inhibition of acid sphingomyelinase by bisphosphonates. *Angew. Chem. Int. Ed. Engl.* **48:** 7560–7563.
65. Kornhuber, J., P. Tripal, M. Reichel, C. Muhle, C. Rhein, M. Muehlbacher, T. W. Groemer, and E. Gulbins. 2010. Functional Inhibitors of Acid Sphingomyelinase (FIASMAs): a novel pharmacological group of drugs with broad clinical applications. *Cell. Physiol. Biochem.* **26:** 9–20.
66. Bortolotti, P., E. Faure, and E. Kipnis. 2018. Inflammasomes in tissue damages and immune disorders after trauma. *Front. Immunol.* **9:** 1900.
67. Yatsiv, I., M. C. Morganti-Kossmann, D. Perez, C. A. Dinarello, D. Novick, M. Rubinstein, V. I. Otto, M. Rancan, T. Kossmann, C. A. Redaelli, et al. 2002. Elevated intracranial IL-18 in humans and mice after traumatic brain injury and evidence of neuroprotective effects of IL-18-binding protein after experimental closed head injury. *J. Cereb. Blood Flow Metab.* **22:** 971–978.
68. Zhou, R., A. S. Yazdi, P. Menu, and J. Tschopp. 2011. A role for mitochondria in NLRP3 inflammasome activation. *Nature.* **469:** 221–225.
69. Schiweck, J., B. J. Eickholt, and K. Murk. 2018. Important shapeshifter: mechanisms allowing astrocytes to respond to the changing nervous system during development, injury and disease. *Front. Cell. Neurosci.* **12:** 261.
70. Gong, S., C. Zheng, M. L. Doughty, K. Losos, N. Didkovsky, U. B. Schambra, N. J. Nowak, A. Joyner, G. Leblanc, M. E. Hatten, et al. 2003. A gene expression atlas of the central nervous system based on bacterial artificial chromosomes. *Nature.* **425:** 917–925.
71. Burda, J. E., A. M. Bernstein, and M. V. Sofroniew. 2016. Astrocyte roles in traumatic brain injury. *Exp. Neurol.* **275:** 305–315.
72. Wanner, I. B., M. A. Anderson, B. Song, J. Levine, A. Fernandez, Z. Gray-Thompson, Y. Ao, and M. V. Sofroniew. 2013. Glial scar borders are formed by newly proliferated, elongated astrocytes that interact to corral inflammatory and fibrotic cells via STAT3-dependent mechanisms after spinal cord injury. *J. Neurosci.* **33:** 12870–12886.
73. Mathias, S., A. Younes, C. C. Kan, I. Orlow, C. Joseph, and R. N. Kolesnick. 1993. Activation of the sphingomyelin signaling pathway in intact EL4 cells and in a cell-free system by IL-1 beta. *Science.* **259**: 519–522.
74. Göggel, R., S. Winoto-Morbach, G. Vielhaber, Y. Imai, K. Lindner, L. Brade, H. Brade, S. Ehlers, A. S. Slutsky, S. Schutze, et al. 2004. PAF-mediated pulmonary edema: a new role for acid sphingomyelinase and ceramide. *Nat. Med.* **10:** 155–160.
75. Bianco, F., C. Perrotta, L. Novellino, M. Francolini, L. Riganti, E. Menna, L. Saglietti, E. H. Schuchman, R. Furlan, E. Clementi, et al. 2009. Acid sphingomyelinase activity triggers microparticle release from glial cells. *EMBO J.* **28:** 1043–1054.
76. Nedergaard, M., B. Ransom, and S. A. Goldman. 2003. New roles for astrocytes: redefining the functional architecture of the brain. *Trends Neurosci.* **26:** 523–530.
77. Peng, W., M. L. Cotrina, X. Han, H. Yu, L. Bekar, L. Blum, T. Takano, G. F. Tian, S. A. Goldman, and M. Nedergaard. 2009. Systemic administration of an antagonist of the ATP-sensitive receptor P2X7 improves recovery after spinal cord injury. *Proc. Natl. Acad. Sci. USA.* **106:** 12489–12493.

78. Erdreich-Epstein, A., L. B. Tran, O. T. Cox, E. Y. Huang, W. E. Laug, H. Shimada, and M. Millard. 2005. Endothelial apoptosis induced by inhibition of integrins alphavbeta3 and alphavbeta5 involves ceramide metabolic pathways. *Blood.* **105:** 4353–4361.
79. Lee, S. W., S. Gajavelli, M. S. Spurlock, C. Andreoni, J. P. de Rivero Vaccari, M. R. Bullock, R. W. Keane, and W. D. Dietrich. 2018. Microglial inflammasome activation in penetrating ballistic-like brain injury. *J. Neurotrauma.* **35:** 1681–1693.
80. Ismael, S., S. Nasoohi, and T. Ishrat. 2018. MCC950, the selective inhibitor of nucleotide oligomerization domain-like receptor protein-3 inflammasome, protects mice against traumatic brain injury. *J. Neurotrauma.* **35:** 1294–1303.
81. Horng, T. 2014. Calcium signaling and mitochondrial destabilization in the triggering of the NLRP3 inflammasome. *Trends Immunol.* **35:** 253–261.
82. Arora, A. S., B. J. Jones, T. C. Patel, S. F. Bronk, and G. J. Gores. 1997. Ceramide induces hepatocyte cell death through disruption of mitochondrial function in the rat. *Hepatology.* **25:** 958–963.
83. Tseng, W. A., T. Thein, K. Kinnunen, K. Lashkari, M. S. Gregory, P. A. D'Amore, and B. R. Ksander. 2013. NLRP3 inflammasome activation in retinal pigment epithelial cells by lysosomal destabilization: implications for age-related macular degeneration. *Invest. Ophthalmol. Vis. Sci.* **54:** 110–120.
84. Pekny, M., C. B. Johansson, C. Eliasson, J. Stakeberg, A. Wallen, T. Perlmann, U. Lendahl, C. Betsholtz, C. H. Berthold, and J. Frisen. 1999. Abnormal reaction to central nervous system injury in mice lacking glial fibrillary acidic protein and vimentin. *J. Cell Biol.* **145:** 503–514.
85. Karimi-Abdolrezaee, S., and R. Billakanti. 2012. Reactive astrogliosis after spinal cord injury-beneficial and detrimental effects. *Mol. Neurobiol.* **46:** 251–264.
86. Maas, A. I., B. Roozenbeek, and G. T. Manley. 2010. Clinical trials in traumatic brain injury: past experience and current developments. *Neurotherapeutics.* **7:** 115–126.
87. Margulies, S., R. Hicks, and Combination Therapies for Traumatic Brain Injury Workshop Leaders. 2009. Combination therapies for traumatic brain injury: prospective considerations. *J. Neurotrauma.* **26:** 925–939.